Title
Analytical 2-Dimensional Model of Nonpolar and Ionic Solvation in Water

Journal
The Journal of Physical Chemistry B, 125(7)

ISSN
1520-6106

Authors
Yadav, Ajeet Kumar
Bandyopadhyay, Pradipta
Urbic, Tomaz
et al.

Publication Date
2021-02-25

DOI
10.1021/acs.jpcb.0c10329

Peer reviewed

HHS Public Access

Author manuscript

J Phys Chem B. Author manuscript; available in PMC 2022 February 25.

Published in final edited form as:

J Phys Chem B. 2021 February 25; 125(7): 1861–1873. doi:10.1021/acs.jpcb.0c10329.

Analytical 2-Dimensional Model of Nonpolar and Ionic Solvation in Water

Ajeet Kumar Yadav,
School of Computational and Integrative Sciences, Jawaharlal Nehru University, New Delhi 110067, India

Pradipta Bandyopadhyay,
School of Computational and Integrative Sciences, Jawaharlal Nehru University, New Delhi 110067, India

Tomaz Urbic,
Faculty of Chemistry and Chemical Technology, University of Ljubljana, SI-1000 Ljubljana, Slovenia

Ken A. Dill
Laufer Center for Physical and Quantitative Biology, Department of Physics and Astronomy, and Department of Chemistry, Stony Brook University, New York 11794, United States

Abstract

A goal in computational chemistry is computing hydration free energies of nonpolar and charged solutes accurately, but with much greater computational speeds than in today's explicit-water simulations. Here, we take one step in that direction: a simple model of solvating waters that is analytical and thus essentially instantaneous to compute. Each water molecule is a 2-dimensional dipolar hydrogen-bonding disk that interacts around small circular solutes with different nonpolar and charge interactions. The model gives good qualitative agreement with experiments. As a function of the solute radius, it gives the solvation free energy, enthalpy and entropy as a function of temperature for the inert gas series Ne, Ar, Kr, and Xe. For anions and cations, it captures relatively well the trends versus ion radius. This approach should be readily generalizable to three dimensions.

Corresponding Author: **Ken A. Dill** – dill@laufercenter.org.

Supporting Information

The Supporting Information is available free of charge at https://pubs.acs.org/doi/10.1021/acs.jpcb.0c10329.

Comparison of theory and simulation for ion solvation thermodynamics and effect of variation of parameters of the model for both nonpolar and ionic cases on thermodynamic properties (PDF)

Complete contact information is available at: https://pubs.acs.org/10.1021/acs.jpcb.0c10329

The authors declare no competing financial interest.

DEDICATION

We offer this work in honor of Dave Thirumalai's 65th birthday. He's been a dear friend, a major community influencer, and one of the most insightful biophysical theorists we know. Thanks, Dave!

NOTE ADDED AFTER ASAP PUBLICATION

This paper was published on February 4, 2021, without its intended dedication note. The corrected version was reposted on February 10, 2021.

Graphical Abstract

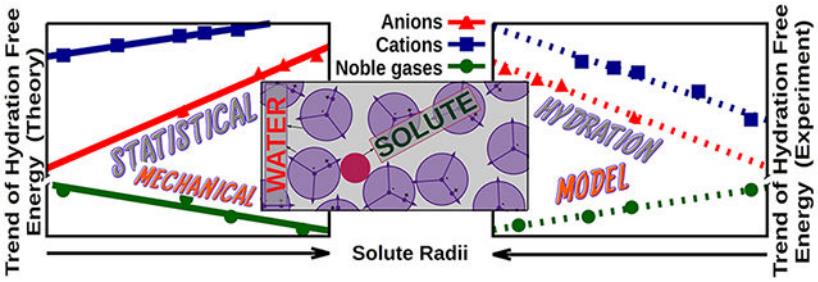

1. INTRODUCTION

Many processes in biology, chemistry, physics, and materials science take place in water.[1] They include protein folding, protein binding to drugs and other ligands, membrane assembly, molecular partitioning between media, and surface adsorption. A driving force common to many of these processes is the solvation and desolvation by water. In each time step as a protein molecule folds, it may bury some hydrophobic surface away from water or expose some ionic amino acid side chain to the solvent. The equilibria, and rates and routes of such steps and processes, depend on the solvation free energy and its thermodynamic components. In order to model these energetic costs accurately in the computer, we need suitable models of physical solvation and desolvation.

Computing solvation free energies has been done using different modeling approaches. One approach is based on measurements of free energies of oil–water transfers of *model compound* small molecules and using additivity relations to sum them.[2] However, because nonadditivities are often large, such model compound approaches are rarely used for quantitative modeling. Second, there are *statistical mechanical* approaches, which can be relatively fast to compute, but they owe their speeds to the use of simplified water geometries that allow averaging using integral equation theory or density functional theories.[3–7]

The second principal approach is to use Molecular Dynamics (MD) simulations with some treatment of water and using force fields that account for the other energetic components. The two main treatments of water are *implicit solvent* and explicit solvent. In *implicit solvation*, water is treated as a continuum, expressing some structural features at less than a full atomistic description.[8–12] Implicit solvation is fast to compute, but it often misses some of the physics (for example, positive and negative ions of the same radius would give the same solvation free energies in a continuum model, in disagreement with chaotropic and kosmotropic effects of ion radii seen in experiments). *Explicit solvent* models, such as the TIP or SPC models[13–25] are the current gold-standard approach for complex processes because they capture the physics fairly well for a wide range of arbitrary systems. But explicit solvation has two principal downsides. First, it has high computational costs, which render calculations of derivative properties, like heat capacities, compressibilities, and structural populations, difficult to converge. Second, because explicit models sample many individual water molecules, there are usually fluctuations, small numbers of trajectories, and

sampling errors. This “noise” interferes with drawing inferences along a logical pipeline from molecular structure to macroscopic properties.

There would be value in a water model that is fast to compute, captures more of the microscopic surface physics, and is close to analytical to allow studies of the thermodynamic properties. The challenge is that every water molecule has three incompatible geometries: the roughly spherical symmetry of its nonpolar interactions, its electrical dipole, and the tetrahedral symmetry of its hydrogen-bonding (H-bonding) interactions. It has been difficult to capture all three within a model that is analytical or fast to compute. We and others have developed analytical models to capture these otherwise incompatible geometric symmetries, based on simplifying other aspects, for pure water[26–30] and for solvation.[31–33] Most recently, this has resulted in the Cage Water Model,[30] which captures two components—the spherical and tetrahedral symmetries—computable with an analytical partition function, which gives the properties of pure liquid water quite accurately as functions of temperature and pressure, in nearly instantaneous calculations.

In the spirit of earlier work,[27] we first develop the approach in a two-dimensional (2D) model, and if it captures sufficient physics, then to treat the greater complexity in 3D. Here, water molecules are represented as disks (in two dimensions) with three arms. The underlying structure is a cage of waters similar to the hexagonal lattice of ice. The interactions among the waters are represented by a set of two-body terms (hydrogen-bonded and Lennard-Jones states), a combination of one-body terms representing the open state and a many-body term representing the cooperative state where all members of the cage interact. Using this model, the partition function of the system is calculated, and then different thermodynamic properties are obtained at different temperatures and pressures. In our solvation model, the underlying water model is same for both hydrophobic and ionic solutes. The presence of a solute (a) perturbs the symmetry of the cage structure (entropic effect) geometrically and (b) introduces a solute–water interaction (enthalpic effect) in the system. Using this physical picture and with only one parameter used to describe the solute–water interaction, we could obtain the correct trend in the thermodynamic properties, such as free energy, enthalpy and entropy of hydration for four inert gases (Ne, Ar, Kr, and Xe) for a large range of temperature. For the ionic solute case, we have introduced a dipole in water[34] and the interaction of solute–water is treated with this ion–dipole interaction. Here also, with only a few parameters, relative hydration free energy, enthalpy, and entropy are calculated for cations and anions and give the correct trend as found in experiments. We have also calculated water structure disruption from our model for the ions, which is in agreement with the extensive simulation of Galamba.[35]

2. METHODS

Model of Pure Water.

This model for pure water originates from the Mercedes-Benz (MB) model of Ben-Naim.[36,37] A simpler version of the model was solved analytically by Truskett and Dill.[26] This model has been improved over the years.[27–30] In this work, we use the 2D version of the model as shown schematically in Figure 1. The model has been described in detail in several publications.[26–30] We are explaining it briefly in this work. This model has its origin in the

cell theory of statistical mechanics:[38] more specifically, in the variable structure cell theory,[26] where different cell types are considered to capture the complex local environment of water. The cells fluctuate between different microscopic structures of water (defined below). As in the cell theory, the total partition function is computed from the partition functions of each cell.

In this theory, each water is modeled as a 2D disk with three H-bonding arms. The underlying lattice of water is hexagonal as in ice and the structure of liquid water is a deviation from that lattice. In that hexagonal cage, waters can exist in different states such as hydrogen-bonded (HB), Lennard-Jones (LJ), open (O), and solid (S), as defined below. From the partition function of the cage, total partition function of the system is calculated. To get the partition function of the cage, one water (the test water) and its clockwise neighbor is considered at a time. The clockwise direction is taken solely for bookkeeping purposes. The partition function of the cage is determined from the partition function of one water. Distance between two waters and how the arms of two waters are located with respect to each other determines the different states of this model. Figure 1 shows the four states in the different panels. Panels 1, 2, 3, and 4 of the figure show the HB, LJ, O, and S states, respectively. If a H-bonding arm of the test water makes an angle with the line joining centers of test water and its clockwise neighboring water within the range $-\frac{\pi}{3}$ to $+\frac{\pi}{3}$ (and one arm of the neighboring water is aligned to the line joining centers of two waters), then it is considered as the HB state. Moreover, two waters should form a van der Waals (VDW) contact in the HB state. If the distance criterion is satisfied but not the orientational one, then the two waters form the LJ state. If neither of distance and orientational criteria is fulfilled, then it is considered as the open (O) state. When all six waters of the hexagonal cage are hydrogen bonded to each other, then each HB state is defined as the solid (S) state.

We use the following procedure. We first calculate the statistical weight of one water molecule. Then we calculate the partition function of the hexagonal cage from that. Finally, we calculate the total partition function of the whole system from the partition function of the cages.

The statistical weight, Δ_j of the jth state of the model in the isobaric–isothermal ensemble is given by eq 1.

$$\Delta_j = c(T) \int\int \mathrm{d}x\, \mathrm{d}y \int_{-\pi/3}^{\pi/3} \exp\left(-\frac{u_j + \frac{2}{3}pv_j}{\mathrm{kT}}\right) \mathrm{d}\theta \tag{1}$$

Here $c(T)$ is the kinetic part of the statisitcal weight.[26] u_j is the energy of interaction between two waters, whose expression is given later, k, T, and p represent the Boltzmann constant, temperature, and pressure, respectively. The double integration over x and y gives the translational freedom one water has over the other water while being in the jth state and has different values for different states. For the HB and S state, it is taken as 0.242, for the LJ state, it is taken as 0.364, and for the open state, it has the value kT/p.[26] v_j is defined as the

volume per molecule of water, which is taken as fixed for a particular state.[26] v_j values are obtained primarily from geometrical consideration and have the following expressions:[27]

$$v_{HB} = 1.1 \times \sqrt{3}\frac{r_{HB}^2}{2}$$

$$v_{LJ} = \frac{\sqrt{3}\sqrt[3]{2}\sigma_{LJ}^2}{2}$$

$$v_O = \frac{kT}{p} + v_{LJ}$$

$$v_S = \frac{3\sqrt{3}r_{HB}^2}{2}$$

Here r_{HB}, σ_{LJ}, and v_{LJ} represent hydrogen bond length, VDW contact distance, and the volume of the LJ state, respectively. The angle θ is defined in Figure 1.

Energies of interaction (u_j) for the HB and LJ states are given below. For the O state, the interaction is zero.

$$u_{HB} = -\varepsilon_{HB} - \varepsilon_{LJ} + k_s\theta^2 \quad \text{for} \quad -\frac{\pi}{3} < \theta < \frac{\pi}{3} \tag{2a}$$

$$u_{LJ} = -\varepsilon_{LJ} \tag{2b}$$

ε_{HB} is the energy representing the maximal strength of a hydrogen bond (H-bond). ε_{LJ} is the Lennard-Jones contact energy between two waters. k_s is the angular force constant of the harmonic potential, given in the last term of eq 2a, characterizing the angle dependence of the H-bond strength as the angle θ changes. The partition function shown in eq 1 is analytically soluble for each of the four states.[26] The partition function of a cage of six waters can be constructed from the individual statistical weights and is given in eq 3

$$Q_1 = (\Delta_{HB} + \Delta_{LJ} + \Delta_O)^6 - \Delta_{HB}^6 + \Delta_S^6 \exp\left(-\frac{\varepsilon_c}{kT}\right) \tag{3}$$

Here the first three terms within the first parentheses come from the HB, LJ, and O states. The fourth term (with the negative sign) subtracts hexagonal water cages that have only the normal weak water–water interaction, so that it can be replaced by the fifth term of cages that have stronger cooperative H-bonds. That is, Δ_s is the statistical weight of the “solid state” (stronger hexagonal cages) and e_c is its cooperativity energy. Finally correlation

between the cages is taken into account using a mean-field approach. In the mean-field approach the interaction between the cages are considered by defining a van der Waals term equal to $-\frac{N_a}{V}$ where a is a constant, N is the total number of water molecules, and V is the molar volume of water. This reduces the pressure p_0 to $p = p_0 - \frac{a}{V^2}$. Correct molar volume at pressure p_0 is determined by an iterative procedure, details of which can be found in ref 26.

From the partition function of a cage, the population of a state j, f_j can be obtained as

$$f_j = \frac{\partial[\ln Q_1]}{\partial\left[\ln \Delta_j^6\right]}$$

The full partition function of the system of N particles is given by

$$Q = (Q_1)^{N/6} \tag{4}$$

Equation 4 takes into account for the three possible interactions per water and corrects the double counting of the H-bonds.

From the partition function, any thermodynamic quantity can be calculated using standard thermodynamic relationships.

Treating Solvation.

We follow the formulation of Luksic et al.[31] in treating solvation of spherical solutes. In this model, partition function of *a water molecule* in the first solvation shell of the solute is calculated both in the bulk and in the presence of a solute. The free energy of transfer is calculated using the ratio of these two partition functions. Other thermodynamic quantities such as entropy and enthalpy of solvation can also be obtained from these two partition functions. The calculation of the partition function involves three steps:

- **a.** Average energy of a water in the bulk state and in the presence of a solute.
- **b.** The change in the number of H-bonds due to the geometrical constraint introduced by the solute.
- **c.** Finally, the evaluation of the partition function using the information from steps a and b.

The average energy of a bulk water in the jth state is determined in the following way;

$$\langle u_j \rangle = \frac{\int_{-\pi/3}^{\pi/3} u_j \exp\left(-\frac{u_j + (2/3)p v_j}{kT}\right) \mathrm{d}\theta}{\int_{-\pi/3}^{\pi/3} \exp\left(-\frac{u_j + (2/3)p v_j}{\mathrm{kT}}\right) \mathrm{d}\theta} \tag{5}$$

The average energy of a water in the bulk can be obtained by summing over the average energies in four different states as

$$\langle \varepsilon \rangle_{\mathrm{b}} = \frac{3}{2}\{\langle u_{\mathrm{HB}} \rangle f_{\mathrm{HB}} + \langle u_{\mathrm{S}} \rangle f_{\mathrm{S}} + \langle u_{\mathrm{LJ}} \rangle f_{\mathrm{LJ}}\} \quad (6)$$

Here f_j are the populations of different states as defined before. The average energy of the open state is not in eq 6 as its value is zero.[31] The factor $\frac{3}{2}$ comes from the fact that each water can make three interactions and there is a double counting of interactions.

The partition function of one water in the bulk is given by

$$q_{\mathrm{b}} = \int_0^{\pi/3} \exp\left(-\frac{\langle \varepsilon \rangle_{\mathrm{b}} + p v_{\mathrm{mol}}^{\mathrm{b}}}{kT}\right) \mathrm{d}\phi \quad (7)$$

where v_{mol}^{b} is the molar volume of water and ϕ is defined in the next section. Other symbols have been defined before.

Geometrical Aspects of Solvation.

The presence of a solute creates a geometrical constraint affecting the number of H-bonds one water can form. This can be seen from Figure 2. The angle ϕ is defined as the angle between a H-bonding arm and the vector joining the centers of water and the solute. The threshold value (ϕ_c) of that angle is when the H-bonding arm is along the tangent to the solute.

ϕ_c can be calculated as (see Figure 2)

$$\phi_c = \arccos\left(\frac{r_{\mathrm{HB}}}{\sigma_{\mathrm{s}} + \sigma_{\mathrm{LJ}}}\right) \quad (8)$$

r_{HB} is the H-bond length. σ_{s} and σ_{LJ} are the diameters of the solute and water, respectively.

The quantity $\xi(\phi)$ is defined as the maximum number of H-bonds formed by a water molecule in the presence of the solute. It is defined as

For smaller solutes ($\phi_c \leq \pi/3$)

$$\xi(\phi) = 2 \text{ for } 0 \leq \phi \leq \phi_c$$

Or

$$\xi(\phi) = 3 \text{ for } \phi_c \leq \phi \leq \pi/3$$

For larger solutes ($\pi/3 < \phi_c \leq \pi/2$)

$$\xi(\phi) = 2 \text{ for } 0 \leq \phi \leq \frac{2\pi}{3} - \phi_c$$

Or

$$\xi(\phi) = 1 \text{ for } \frac{2\pi}{3} \leq \phi_c \leq \frac{\pi}{3}$$

The average energy of a water in the presence of a solute can be obtained using the following equation.

$$\langle \varepsilon(\xi(\phi)) \rangle_h = \frac{1}{2}\{\xi(\phi)[\langle u_{HB} \rangle f_{HB} + \langle u_S \rangle f_S] + 3\langle u_{LJ} \rangle f_{LJ} - \varepsilon_{sw}\} \quad (9)$$

As can be seen from the above equation is that $\xi(\phi)$ represents the number of H-bonds possible in the presence of a solute and affects the HB and S states. There is a new term ε_{sw}, which represents the interaction between solute and water. It is to be noted that the population of different states are taken as same for both bulk water and water in the presence of a solute in our model.

Calculation of Average Energy of a Water in the Presence of a Solute.

The calculation of the average energy of a water in the presence of the solute differs between hydrophobic and polar solutes, which is described below.

Hydrophobic Solute.—The energy of interaction (ε_{sw}) between a water and the solute is taken as a scalar (u_{np}).

Polar Solute.—Figure 3 shows the model for interaction between an ion and a water molecule. The water charges are represented by a dipole on one of the arms of water. The negative charge is kept at the center of the disk, and the positive charge is kept closer to the surface with a distance 0.185, in reduced unit (defined later), from the center.[34] This is coming from the fact that the water charge density is asymmetric and the positive charge is closer to the surface of water. This dipolar description can be termed as a two-site model of water. The interaction between the ion and the charges of water are given by an empirical energy function as

$$u_{elec} = \eta\left(\frac{q_s q_p}{r_{sp}^2} + \frac{q_s q_n}{r_{sn}^2}\right) \quad (10)$$

where the q_s, q_p, and q_n represent solute charge, positive and negative charge of water, respectively. r_{sp} (r_{sn}) is the distance between the solute and the positive charge (negative charge) of water, η is a parameter having the unit of length.

Here is the reason for the $1/r^2$ distance dependence of charges in eq 10. Although in 2D a logarithmic dependence on r is present according to Coulomb's law, we modeled the electrostatics with an expression consistent with a 3D case. Instead of using a Yukawa potential as used in ref 34, we used a function with $1/r^2$ distance-dependence to capture the faster decay of the interaction with distance (akin to Yukawa potential) than a pure Columbic decay. The value of η was taken as 0.25 after some trials.

The average energy of the electrostatics interaction between water–ion is given by

$$\langle u_{\text{elec}} \rangle = \frac{\int_a^b u_{\text{elec}} \exp(-\beta(u_{\text{elec}} + pv)r \, \mathrm{d}r \, \mathrm{d}\theta}{\int_a^b \exp(-\beta(u_{\text{elec}} + pv)r \, \mathrm{d}r \, \mathrm{d}\theta} \tag{11}$$

The limits of integration *"a"* is the distance between a charge on water and the ion, when the ion touches the water. The upper limit of integration *"b"* is a parameter which we have tested with different values remembering that we are capturing the first-solvation shell effect of the solute. We have eventually taken a+0.5, in reduced unit, as the value of b. The integrand does not lead to zero at that distance, which indicates that the electrostatic effects, based on this model, are present beyond the first solvation shell. This is taken care by the other parameters of the model.

Equation 11 can be simplified to

$$\langle u_{\text{elec}} \rangle = \frac{kT \int_a^b \frac{a}{r} \exp\left(-\frac{a}{r^2}\right) \mathrm{d}r}{\int_a^b \exp\left(-\frac{a}{r^2}\right) r \, \mathrm{d}r} \tag{12}$$

where $\alpha = \frac{\eta q_i q_j}{kT}$ and the subscript on r is omitted.

The above integration has the solution

$$\langle u_{\text{elec}} \rangle = \frac{-kT(\alpha E_{\text{i}}\left(-\frac{\alpha}{r^2}\right) + C}{\left(r^2 \exp\left(-\frac{\alpha}{r^2}\right) + \alpha E_{\text{i}}\left(-\frac{\alpha}{r^2}\right)\right) + C} \tag{13}$$

where E_{i} denotes the exponential integral and C is the constant of integration.

Unlike the hydrophobic case, the disruption of H-bonding is caused not only by the size of the solute but also by the charge density of the solute in a nontrivial way. To take care of this, we have multiplied $\xi(\phi)$, which is defined in the previous section, by a function

$$\text{factor} = \left(\frac{1}{\rho}\right)^{\delta} \tag{14}$$

where ρ is the charge density of the solute and δ is a parameter. ε_{sw} is taken as a sum of u_{np} and $\langle u_{\text{elec}} \rangle$. Finally, we use a factor γ to multiply the total electrostatic energy to get the energy values of H-bonding and electrostatics comparable. All of these are put into eq 9 to calculate the average energy of a water in the presence of a solute. The parameters of the model are (1) "b", the upper limit of integration, (2) δ to describe the disruption of H-bonding, and (3) γ to make the energy of different terms comparable.

Calculation of Thermodynamic Quantities in Solvation.

Partition function of a water in the presence of a solute is calculated in the same way as in eq 7.

$$q_{\mathrm{h}} = \int_0^{\pi/3} \exp\left(-\frac{\langle \varepsilon(\xi(\phi))\rangle_{\mathrm{h}} + p v_{\mathrm{mol}}^{\mathrm{h}}}{kT}\right) \mathrm{d}\phi \tag{15}$$

There are two changes: (a) the average energy of a water is different between that in the bulk and that in the presence of a solute, and (b) the molar volume of water in the presence of solute is different and it has been estimated in the same way as done in ref 31. Finally, the Gibbs free energy of transferring a solute to water is given by

$$\Delta G = -n(\sigma_s)kT \ln\left(\frac{q_{\mathrm{h}}}{q_{\mathrm{b}}}\right) \tag{16}$$

where $n(\sigma_{\mathrm{s}})$ is the average number of water molecules in the solvation shell of the solute, calculated in the same way as in ref 31. Enthalpy and entropy are calculated from the following standard expressions.

$$\Delta H = n(\sigma_{\mathrm{s}})kT^2 \frac{\partial\left(\ln\left(\frac{q_{\mathrm{h}}}{q_{\mathrm{b}}}\right)\right)}{\partial T} \tag{17}$$

$$T\Delta S = \Delta H - \Delta G \tag{18}$$

Parameters Used in the Calculation.

Pure Water.—We have taken the same parameters as used in ref 27. The parameters are as follows: $\varepsilon_{\mathrm{HB}} = 1$, $r_{\mathrm{HB}} = 1$, $\varepsilon_{\mathrm{LJ}} = 0.1$, $\sigma_{\mathrm{LJ}} = 0.7$, $k_{\mathrm{s}} = 10$, and $\varepsilon_{\mathrm{c}} = 0.06$. All calculations were done in reduced units, such as, temperature, $T^* = kT/|\varepsilon_{\mathrm{HB}}|$, $G^* = G/|\varepsilon_{\mathrm{HB}}|$, $H^* = H/|\varepsilon_{\mathrm{HB}}|$, $\mathrm{TS}^* = \mathrm{TS}/|\varepsilon_{\mathrm{HB}}|$. All distances are scaled by r_{HB}; i.e., $\sigma_{\mathrm{LJ}} = 0.7$ means $\sigma_{\mathrm{LJ}} = 0.7 r_{\mathrm{HB}}$.

Nonpolar Solutes.—$\varepsilon_{\mathrm{sw}}$ of different noble gases have been parametrized to reproduce the experimental thermodynamic quantities. ε_{sw} is taken as 0.22, 0.30, 0.37, and 0.43 for Ne, Ar, Kr, and Xe, respectively. Each term is scaled with a division by square root of kT. The radii of the inert gases are taken from the work of Vogt et al.[39]

Ions.—δ and γ are taken to be 0.3 and 6.0, respectively. We take the radii of the ions as the crystal radii from ref 34 (Table 1). The calculation for Li^+ is done in the following way: as eq 8 is not valid for a diameter less than $0.3 r_{\mathrm{HB}}$ (diameter of Li^+ is $0.24 r_{\mathrm{HB}}$), we have used the value $0.3 r_{\mathrm{HB}}$ while using eq 8. However, for electrostatics interaction, a diameter of $0.24 r_{\mathrm{HB}}$ is used.

All calculated values below are put into reduced units. We have made no attempt to rescale these to the experimental energy and temperature scales, because any agreement of this 2D model with 3D experimental reality would only come from gratuitous parameter fitting. Our goal here is to see if we capture the physical trends.

3. RESULTS

Hydration Thermodynamics of the Inert Gas Nonpolar Solutes.

Figures 4–6 show both the calculated and experimental hydration free energies, enthalpies and entropies[40] as a function of temperature for the four inert gases, Ne, Ar, Kr, and Xe. The trends with temperature are correct, and the effects of solute size are also captured reasonably well. Larger inert gas atoms are more soluble than smaller ones (i.e., the hydration free energy becomes less positive for larger sizes).[41] Figure 5 shows that this is because the hydration enthalpy is more favorable for the larger solutes and because the enthalpy dominates over the entropy (Figure 6). Our energy parameters for the inert gases are proportional to their sizes. With this energy parameter we are able to reproduce the trend in enthalpy, which, in conjunction with the correct trend in entropy given by our model, also gives the correct trend in free energy of solvation. Figure 7 shows these same thermodynamic quantities, but plotted now as a function of solute radius, for a fixed temperature.

Here is the microscopic interpretation of these results in terms of the model. First, these inert gas atoms are all nonpolar. They prefer not to be dissolved in water in the first place. Second, cold water is relatively cage-like. Inserting a nonpolar solute into cold water is enthalpically favorable, but it tightens up the first-shell water–water hydrogen bonding, which is entropically unfavorable. Hotter water is looser and less cage-like. So inserting a nonpolar solute into hot water is less enthalpically favorable and causes less ordering of the surrounding waters. This is consistent with the description of Graziano,[41] who frames hydrophobic hydration in terms of direct and indirect effects. In the direct part, inserting the solute causes a loss of configurational freedom of cold water due to the cavity formation, and the direct interaction between the solute and water contributes to the enthalpic part. In the indirect part, the water reorganization contributes to both entropy and enthalpy. In the present model, these effects are due to the loss of the HB state with increasing temperature and gain of LJ and open state populations.[33]

Hydration Thermodynamics of Small Atomic Ions.

Figures 8 and 9 show our calculations of solvation free energy, enthalpy, and entropy compared to experiments, for anions and cations, respectively (see also Table 1). The model gives the correct qualitative trends with all the properties, size, and charge sign.

Here is the model explanation of the trends. First, for all anions and cations, dissolving in water is favorable. The free energy of solvation is negative. Second, smaller ions have a stronger drive to dissolve than bigger ions have. Third, for all anions and cations this dissolution process is driven by the enthalpy and opposed by the entropy. This is an effect of charge density. Small ions have high charge density. Higher charge density means more

electrostriction, i.e., a tighter solvation shell of waters, and thus also more water ordering, around the smaller ions. Fourth, cations follow exactly same trends. But, there is a large offset between anions and cations. An anion of a given radius is much more strongly solvating than a cation of the same radius. This offset has long been recognized in the experiments.[42] This can also be seen from Table 1: the radii of F^- and K^+ are almost same, but the hydration free energy is much more favorable for F^-. From Figures 8 and 9, it can be seen that free energy hydration of F^- calculated from our model is much more favorable than that of K^+, although the difference cannot be quantitatively compared with experiments.

For the cations, both experimental ΔG and ΔH values on going from Li^+ to K^+ increase substantially as can be seen from Figure 9. After that, the changes are more gradual. In our model, the large change in ΔG in going from Li^+ to K^+ is captured. For ΔH also, the large change was captured although not completely proportional to experiments. After Na^+, the change of values for other ions are nicely captured. The change from Na^+ to K^+ is more than that from K^+ to Rb^+ and Rb^+ to Cs^+.

These experimental observations that charge density controls ion solvation thermodynamics have been known for many years.[43] Ions that cause water ordering (in terms of the solvation entropy and other structural properties) are called *kosmotropes* and ions that disorder water are called *chaotropes*. However, the classification of ions as pure kosmotropes or chaotropes has been criticized as some ions, such as Na+, may act both kosmotropes and chaotropes.[43] The ordering of waters does not say, directly, on the number of H-bonds among waters, although it is expected to decrease with the increase of water ordering around an ion. In our calculation, it is possible to calculate water–water H-bonds in the absence and presence of solute. In a previous work, based on computer simulations and Raman spectroscopy suggested that the main changes in the water network caused by the ions are essentially confined to the first solvation shell.[44] An extensive computer simulation study in ref 35 found that there is change of donor (for anions) and acceptor (for cations) H-bonds around ion in the first solvation shell. Our model considers change of H-bond between waters in the first solvation shell. Our results, although based on a simple picture, correctly predict this trend in terms of total number of H-bonds. For the anions the number of H-bonds per water is 1.32, 1.47, 1.52, and 1.58, for F^-, Cl^-, Br^-, and I^-, respectively. For the cations, this is 1.02, 1.17, 1.31, 1.36, and 1.43 for Li^+, Na^+, K^+, Rb^+, and Cs^+, respectively. However, the difference between different ions is small in our results. In our model, the H-bond among waters changes (a) due to geometric constraint with larger solutes causing more reduction of H-bonds, and (b) due to charge density of the ions, smaller ions being more effective in this case. Hence, two opposite effects, the size and the charge density play a role in reducing the H-bonding among water molecules. The charge density part wins as smaller ions order waters more in their first solvation shell with larger decrease of H-bonding as found by extensive simulation by Galamba et al.[35] Our model also correctly predicts that the effect of charge density overcomes the size effect, and hence, the smaller ions disrupt the H-bonding of waters more. However, because of the specific parameters used the differences between different solutes is smaller than what found in simulation and a comparison between the cations and the anions is not possible.

Next, we investigate the effect of systematic variation of the model parameters for the nonpolar interactions between solute-water, parameters δ and γ for the ions on the thermodynamic quantities calculated for the solutes. We found that, (i) for the inert gases, the water-solute interactions should be roughly proportional to the surface area of the solutes to reproduce the correct trend in the thermodynamic quantities (Figures S7–S9) and, (ii) for the ionic case, the balance between the parameters δ and γ is key to get correct trends in both hydration thermodynamics and water–water H-bonds. Increasing γ (which gives a larger contribution of the electrostatic part of the water–solute interaction to the total average energy of a water) lowers the values of thermodynamic quantities, while the trends among different ions do not change (Figure 10–12). On the other hand, decreasing δ increases the "factor" in eq 14, leading to an increased number of H-bonds one water can make in its solvation shell. This, in turn, makes the average energy of a water in its solvation shell more negative resulting in more negative values for the thermodynamic quantities calculated. Hence, with the decrease of δ. The values of thermodynamic quanties decrease (Figure 13–15). The increase of H-bonds with the decrease of δ is found to be inversely proportional to the ion sizes. This eventually (for δ equals to 0.1) gives a monotonic reduction of average number of H-bonds per water with the increase of the size of the ions (Figure S6) in contradiction with the findings in reference.[35]

4. CONCLUSIONS

We have presented a simple analytical two-dimensional model of nonpolar and ionic solvation. The point of it is to serve as a workbench for exploring fast analytical potential functions, as a stepping stone toward better practical 3D models of solvation components in MD modeling. While it aims to have the speed and scaling behavior of implicit-solvent models, the present work goes beyond current implicit modeling in giving better microscopic physics of solvated surfaces, and it allows for analytical computations of temperature and pressure dependences. It gives good qualitative agreement with experiments of solvation free energy, enthalpy, and entropy as functions of temperature and solute size for nonpolar solutes and in addition for charge sign for ions. Because the model is analytical, it requires almost no computer time. A typical evaluation of all thermodynamic quantities at one temperature took 0.1 s on a desktop computer using a python code, whereas molecular dynamics simulation of Na^+ with about 8000 water molecules of 10 ns takes 3000 s in a GPU-based computer.

Supplementary Material

Refer to Web version on PubMed Central for supplementary material.

ACKNOWLEDGMENTS

Part of this work was done during the sabbatical visit of P.B. to the Laufer Center for Physical and Quantitative Biology at Stony Brook University. P.B. wishes to thank the Laufer center for financial support. K.A.D. appreciates the support of the Laufer Center.

REFERENCES

(1). Brini E; Fennell CJ; Fernandez-Serra M; Hribar-Lee B; Lukšič M; Dill KA How Water's Properties Are Encoded in Its Molecular Structure and Energies. Chem. Rev 2017, 117, 12385–12414. [PubMed: 28949513]

(2). Hermann RB Theory of Hydrophobic Bonding. II. The Correlation of Hydrocarbon Solubility in Water with Solvent Cavity Surface Area. J. Phys. Chem 1972, 76, 2754–2759.

(3). Urbič T; Vlachy V; Kalyuzhnyi YV; Southall NT; Dill KA A Two-Dimensional Model of Water: Solvation of Nonpolar Solutes. J. Chem. Phys 2002, 116, 723–729.

(4). Urbič T; Vlachy V; Kalyuzhnyi YV; Dill KA Orientation-Dependent Integral Equation Theory for a Two-Dimensional Model of Water. J. Chem. Phys 2003, 118, 5516–5525.

(5). Urbic T; Vlachy V; Kalyuzhnyi YV; Dill KA Theory for the Solvation of Nonpolar Solutes in Water. J. Chem. Phys 2007, 127, 174505. [PubMed: 17994825]

(6). Kinoshita M Molecular Origin of the Hydrophobic Effect: Analysis Using the Angle-Dependent Integral Equation Theory. J. Chem. Phys 2008, 128, 024507. [PubMed: 18205459]

(7). Luukkonen S; Levesque M; Belloni L; Borgis D Hydration Free Energies and Solvation Structures with Molecular Density Functional Theory in the Hypernetted Chain Approximation. J. Chem. Phys 2020, 152, 064110. [PubMed: 32061236]

(8). Dzubiella J; Swanson JMJ; McCammon JA Coupling Hydrophobicity, Dispersion, and Electrostatics in Continuum Solvent Models. Phys. Rev. Lett 2006, 96, 087802. [PubMed: 16606226]

(9). Yu Z; Jacobson MP; Josovitz J; Rapp CS; Friesner RA First-Shell Solvation of Ion Pairs: Correction of Systematic Errors in Implicit Solvent Models. J. Phys. Chem. B 2004, 108, 6643–6654.

(10). Topol IA; Tawa GJ; Burt SK; Rashin AA On the Structure and Thermodynamics of Solvated Monoatomic Ions Using a Hybrid Solvation Model. J. Chem. Phys 1999, 111, 10998–11014.

(11). Bandyopadhyay P; Gordon MS; Mennucci B; Tomasi J An Integrated Effective Fragment-Polarizable Continuum Approach to Solvation: Theory and Application to Glycine. J. Chem. Phys 2002, 116, 5023–5032.

(12). Bandyopadhyay P; Gordon MS A Combined Discrete/Continuum Solvation Model: Application to Glycine. J. Chem. Phys 2000, 113, 1104–1109.

(13). Guillot B; Guissani Y A Computer Simulation Study of the Temperature Dependence of the Hydrophobic Hydration. J. Chem. Phys 1993, 99, 8075–8094.

(14). Tanaka H; Nakanishi K Molecular Dynamics Simulations on Aqueous Solutions of Rare Gases. Mol. Simul 1991, 6, 311–324.

(15). Moghaddam MS; Chan HS Pressure and Temperature Dependence of Hydrophobic Hydration: Volumetric, Compressibility, and Thermodynamic Signatures. J. Chem. Phys 2007, 126, 114507. [PubMed: 17381220]

(16). Cerdeiriña CA; Debenedetti PG Water Anomalous Thermodynamics, Attraction, Repulsion, and Hydrophobic Hydration. J. Chem. Phys 2016, 144, 164501. [PubMed: 27131551]

(17). Lee Warren G; Patel S Hydration Free Energies of Monovalent Ions in Transferable Intermolecular Potential Four Point Fluctuating Charge Water: An Assessment of Simulation Methodology and Force Field Performance and Transferability. J. Chem. Phys 2007, 127, 064509. [PubMed: 17705614]

(18). Hummer G; Pratt LR; Garcia AE Free Energy of Ionic Hydration. J. Phys. Chem 1996, 100, 1206–1215.

(19). Tanaka H; Nakanishi K Hydrophobic Hydration of Inert Gases: Thermodynamic Properties, Inherent Structures, and Normal-Mode Analysis. J. Chem. Phys 1991, 95, 3719–3727.

(20). Dowdle JR; Buldyrev SV; Stanley HE; Debenedetti PG; Rossky PJ Temperature and Length Scale Dependence of Solvophobic Solvation in a Single-Site Water-like Liquid. J. Chem. Phys 2013, 138, 064506. [PubMed: 23425478]

(21). Irudayam SJ; Henchman RH Solvation Theory to Provide a Molecular Interpretation of the Hydrophobic Entropy Loss of Noble-Gas Hydration. J. Phys.: Condens. Matter 2010, 22, 284108. [PubMed: 21399280]

(22). Pascal TA; Lin ST; Goddard W; Jung Y Stability of Positively Charged Solutes in Water: A Transition from Hydrophobic to Hydrophilic. J. Phys. Chem. Lett 2012, 3, 294–298. [PubMed: 26285842]

(23). Kuffel A; Zielkiewicz J Why the Solvation Water around Proteins Is More Dense than Bulk Water. J. Phys. Chem. B 2012, 116, 12113–12124. [PubMed: 22998120]

(24). Gerogiokas G; Calabro G; Henchman RH; Southey MWY; Law RJ; Michel J Prediction of Small Molecule Hydration Thermodynamics with Grid Cell Theory. J. Chem. Theory Comput 2014, 10, 35–48. [PubMed: 26579889]

(25). Misin M; Fedorov MV; Palmer DS Hydration Free Energies of Molecular Ions from Theory and Simulation. J. Phys. Chem. B 2016, 120, 975–983. [PubMed: 26756333]

(26). Truskett TM; Dill KA A Simple Statistical Mechanical Model of Water. J. Phys. Chem. B 2002, 106, 11829–11842.

(27). Urbic T; Dill KA A Statistical Mechanical Theory for a Two-Dimensional Model of Water. J. Chem. Phys 2010, 132, 224507. [PubMed: 20550408]

(28). Truskett TM; Dill KA Predicting Water's Phase Diagram and Liquid-State Anomalies. J. Chem. Phys 2002, 117, 5101–5104.

(29). Urbic T Analytical Model for Three-Dimensional Mercedes-Benz Water Molecules. Phys. Rev. E - Stat. Nonlinear Soft Matter Phys 2012, 85, 061503.

(30). Urbic T; Dill KA Water Is a Cagey Liquid. J. Am. Chem. Soc 2018, 140, 17106–17113. [PubMed: 30461279]

(31). Lukšič M; Urbic T; Hribar-Lee B; Dill KA Simple Model of Hydrophobic Hydration. J. Phys. Chem. B 2012, 116, 6177–6186. [PubMed: 22564051]

(32). Xu H; Dill KA Water's Hydrogen Bonds in the Hydrophobic Effect: A Simple Model. J. Phys. Chem. B 2005, 109, 23611–23617. [PubMed: 16375338]

(33). Urbic T; Dill KA Analytical Theory of the Hydrophobic Effect of Solutes in Water. Phys. Rev. E: Stat. Phys., Plasmas, Fluids, Relat. Interdiscip. Top 2017, 96, 032101.

(34). Hribar B; Southall NT; Vlachy V; Dill KA How Ions Affect the Structure of Water. J. Am. Chem. Soc 2002, 124, 12302–12311. [PubMed: 12371874]

(35). Galamba N On the Effects of Temperature, Pressure, and Dissolved Salts on the Hydrogen-Bond Network of Water. J. Phys. Chem. B 2013, 117, 589–601. [PubMed: 23259864]

(36). Ben-Naim A Statistical Mechanics of "waterlike" Particles in Two Dimensions. I. Physical Model and Application of the Percus-Yevick Equation . J. Chem. Phys 1971, 54, 3682–3695.

(37). Ben-Naim A Statistical Mechanics of Water-like Particles in Two-Dimensions: II. One Component System. Mol. Phys 1972, 24, 705–721.

(38). Mayer JE; Mayer MG Statistical Mechanics; John Wiley & Sons Inc.: New York, 1940.

(39). Vogt J; Alvarez S Van Der Waals Radii of Noble Gases. Inorg. Chem 2014, 53, 9260–9266. [PubMed: 25144450]

(40). Crovetto R; Fernandez-Prini R; Japas ML Solubilities of Inert Gases and Methane in H2O and in D 2O in the Temperature Range of 300 to 600 K. J. Chem. Phys 1982, 76, 1077–1086.

(41). Graziano G Comment on "The Mechanism of Hydrophobic Solvation Depends on Solute Radius" J. Phys. Chem. B 2000, 104, 1326.J. Phys. Chem. B 2001, 105, 2079;J. Phys. Chem. B 2001, 105, 2079–2081.

(42). Collins KD; Neilson GW; Enderby JE Ions in water: Characterizing the forces that control chemical processes and biological structure. Biophys. Chem 2007, 128, 95–104. [PubMed: 17418479]

(43). Collins KD Charge density-dependent strength of hydration and biological structure. Biophys. J 1997, 72, 65–76. [PubMed: 8994593]

(44). Smith JD; Saykally RJ; Geissler PL The Effects of Dissolved Halide Anions on Hydrogen Bonding in Liquid Water. J. Am. Chem. Soc 2007, 129, 13847–13856. [PubMed: 17958418]

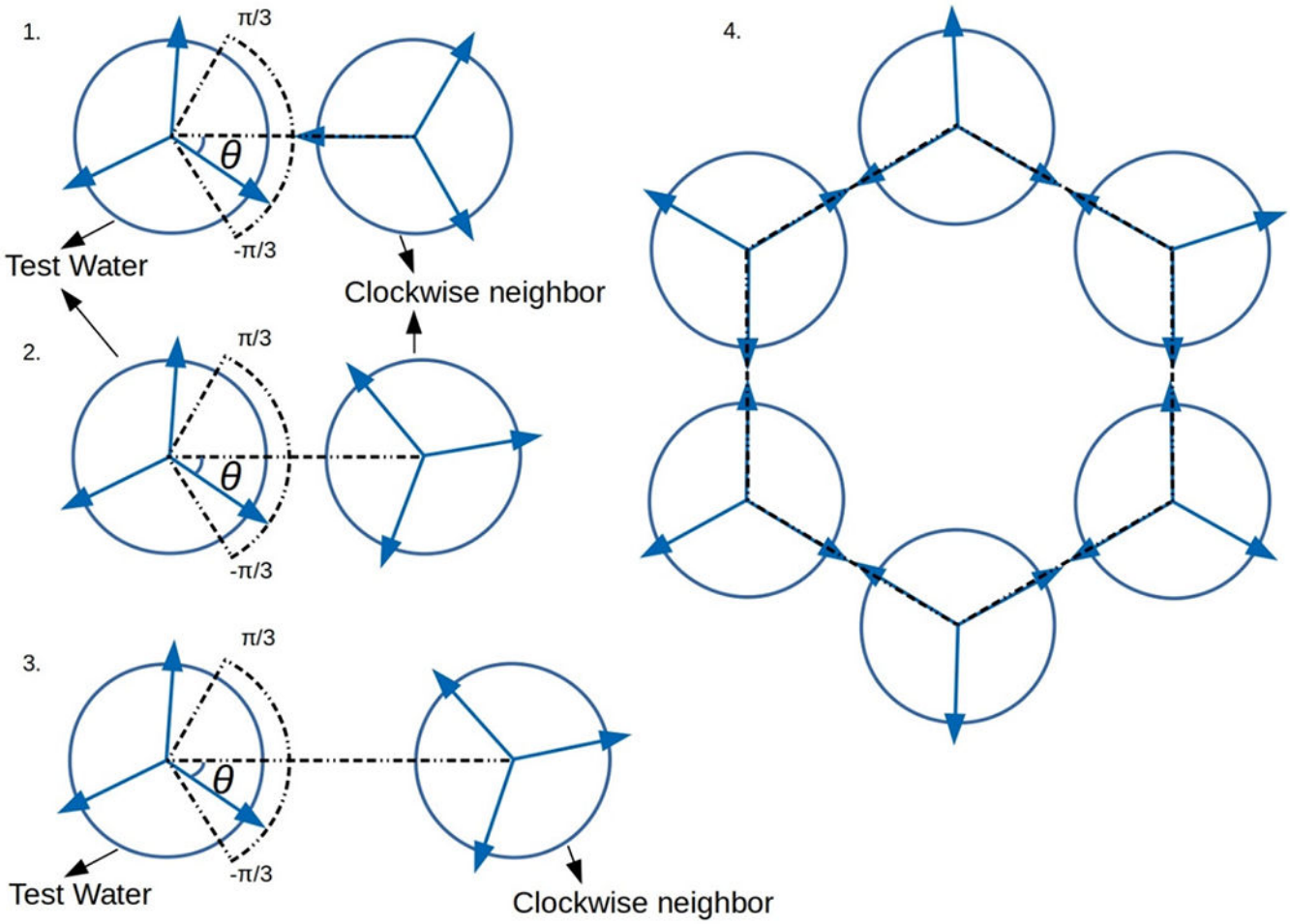

Figure 1.
Different interaction states of the water model: (1) HB state, (2) LJ state, (3) open state, and (4) solid state.

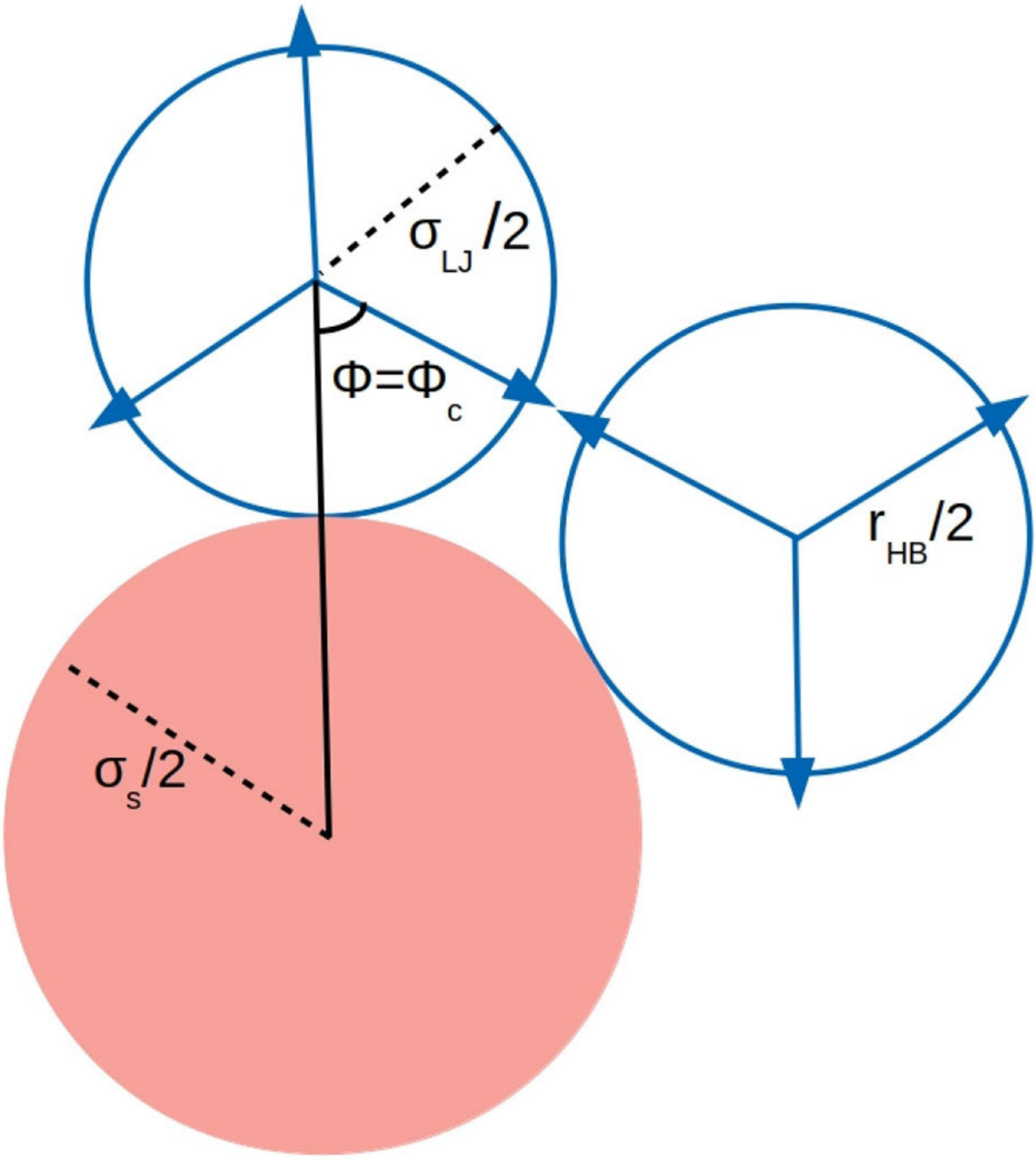

Figure 2.
Definition of the critical angle ϕ_c. The shaded circle is the solute; other circles are water.

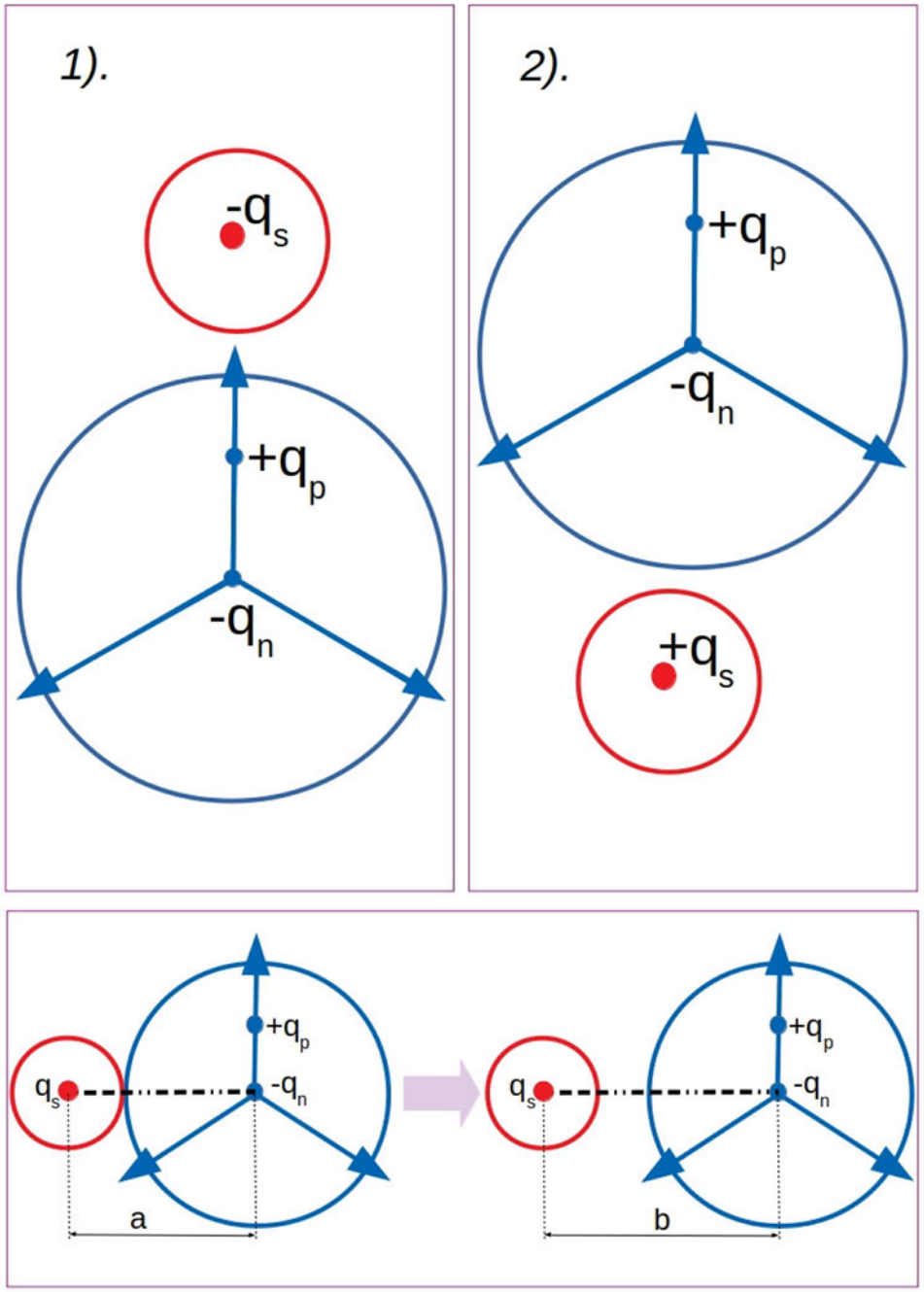

Figure 3.
Top Panel: Approach of (1) anion and (2) cation to a water in the ionic model. Water dipole is also shown. Bottom Panel: Range of integration limits (see eq 11) *a* and *b* are shown.

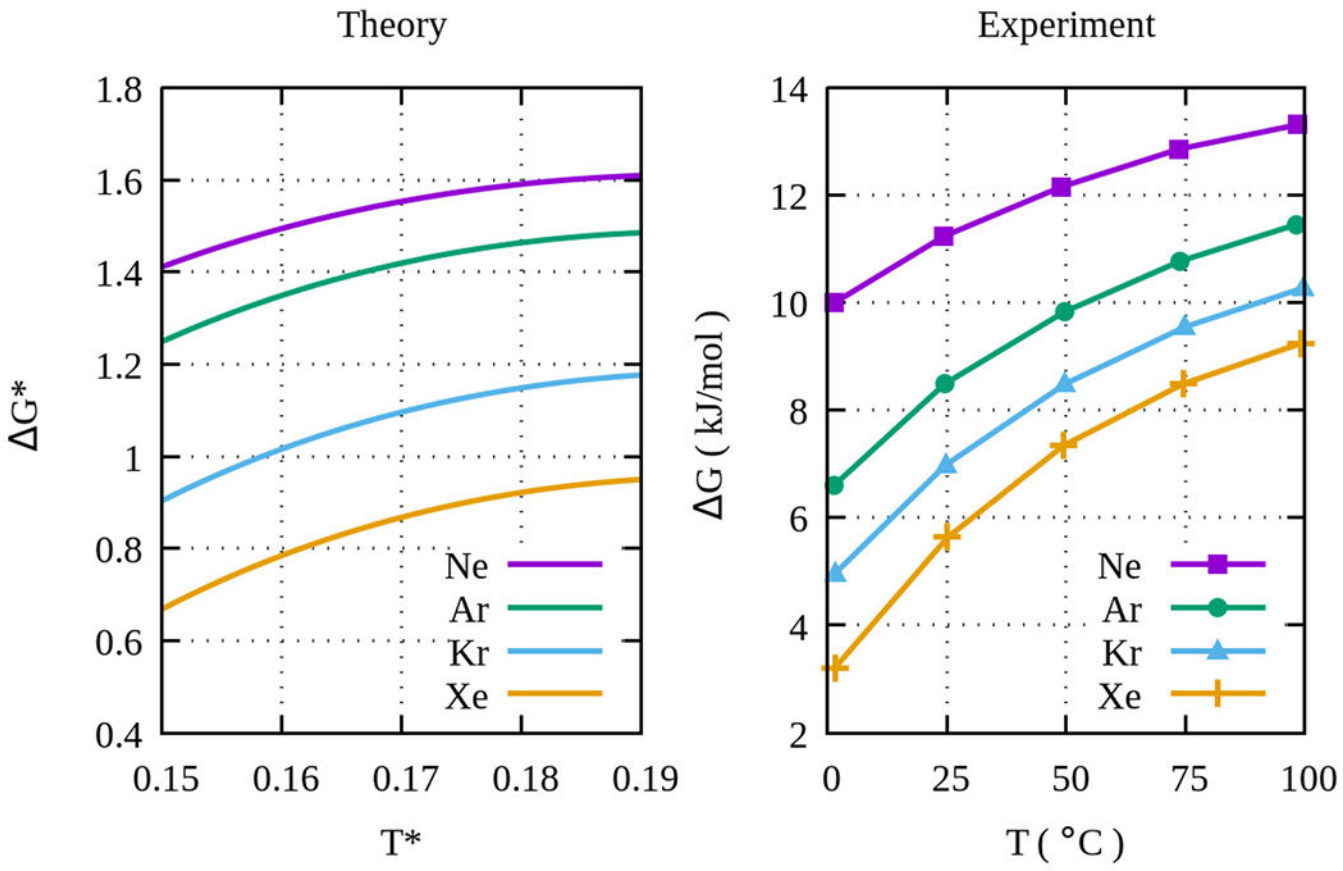

Figure 4.

Hydration free energies of the inert gases, vs temperature, for the different types of gas atoms, which have different radii. The unit of results from the theory is in reduced unit (see text).

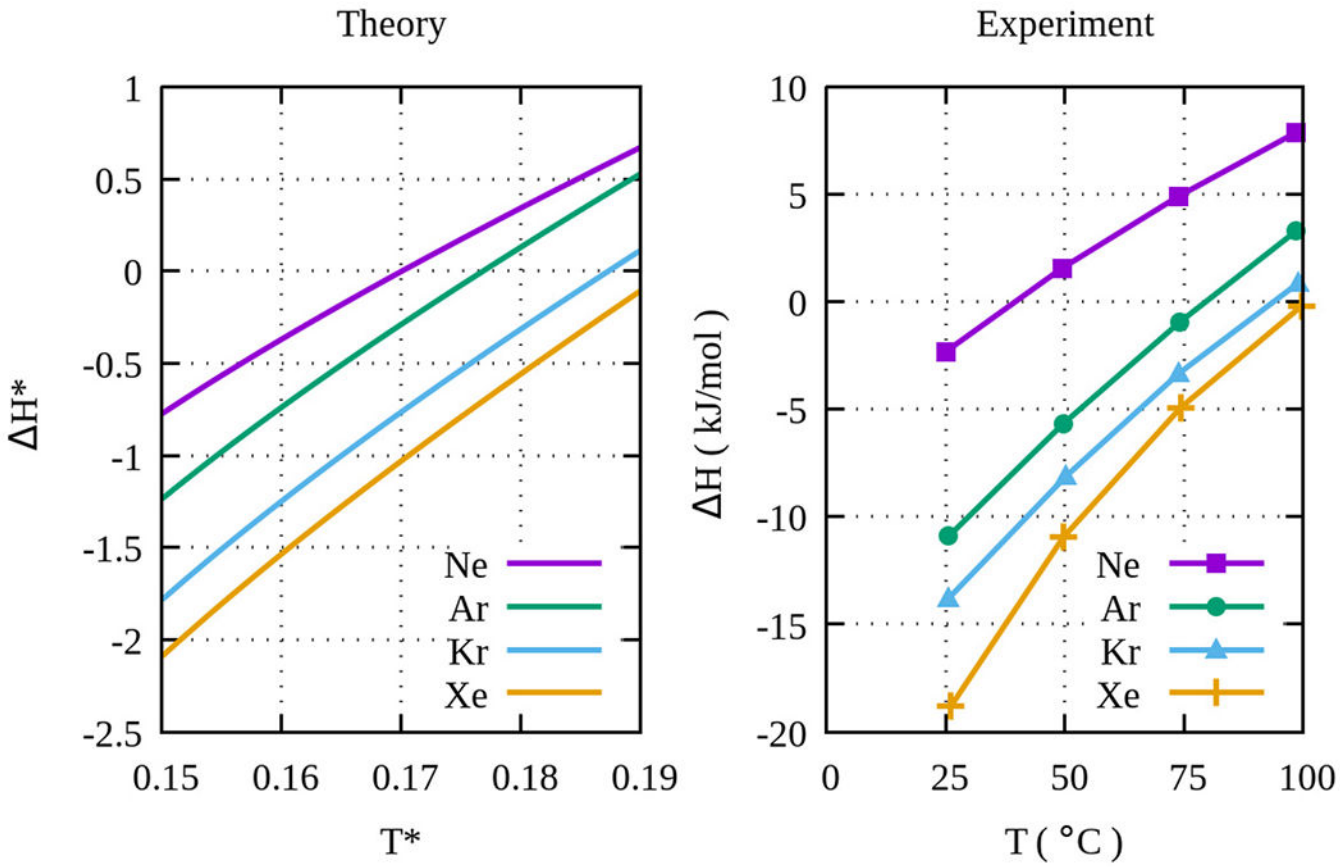

Figure 5.

Hydration enthalpies of the inert gases, vs temperature, for the different types of gas atoms, which have different radii. The unit of results from the theory is in reduced unit (see text).

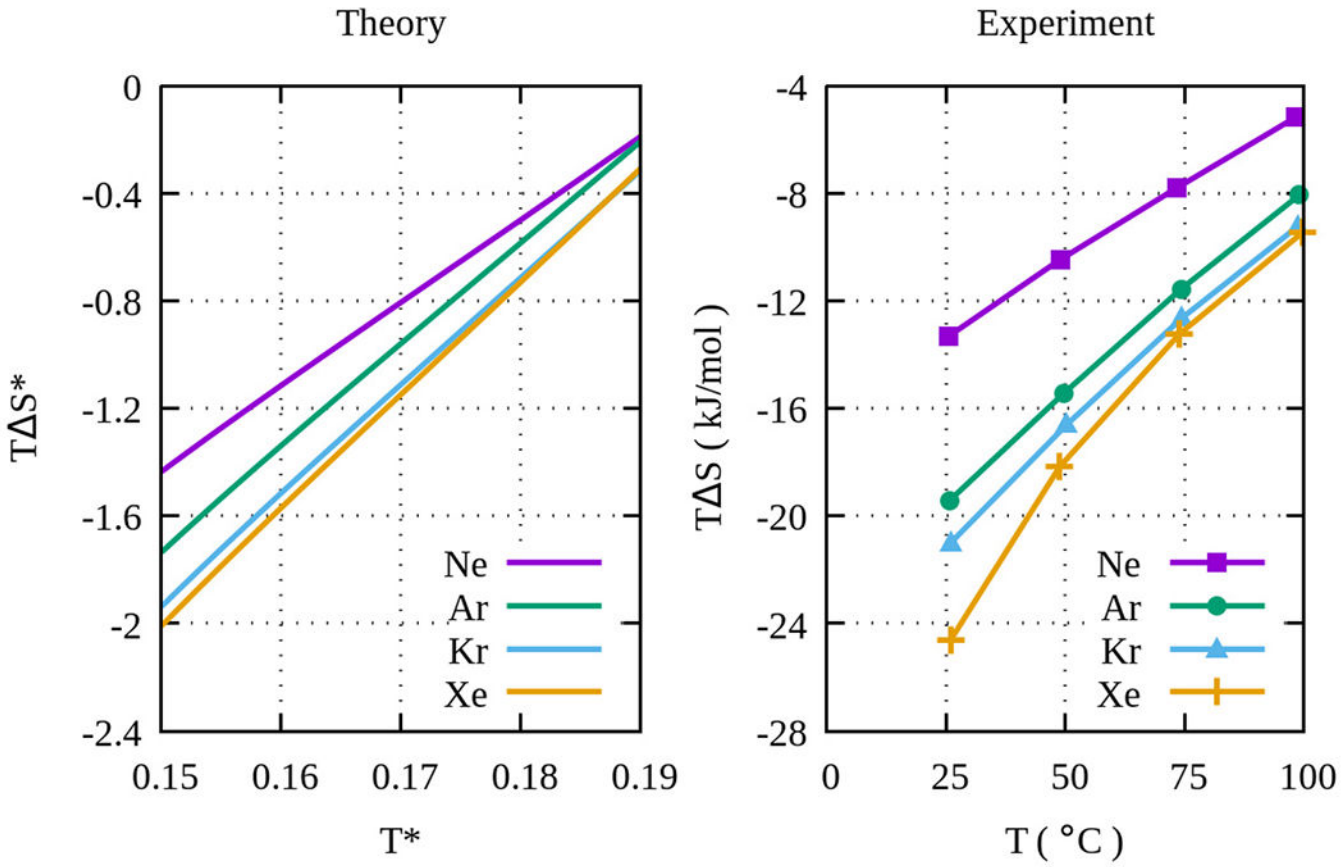

Figure 6.

Hydration entropies multiplied by temperature of the inert gases, vs temperature, for the different types of gas atoms, which have different radii. The unit of results from the theory is in reduced unit (see text).

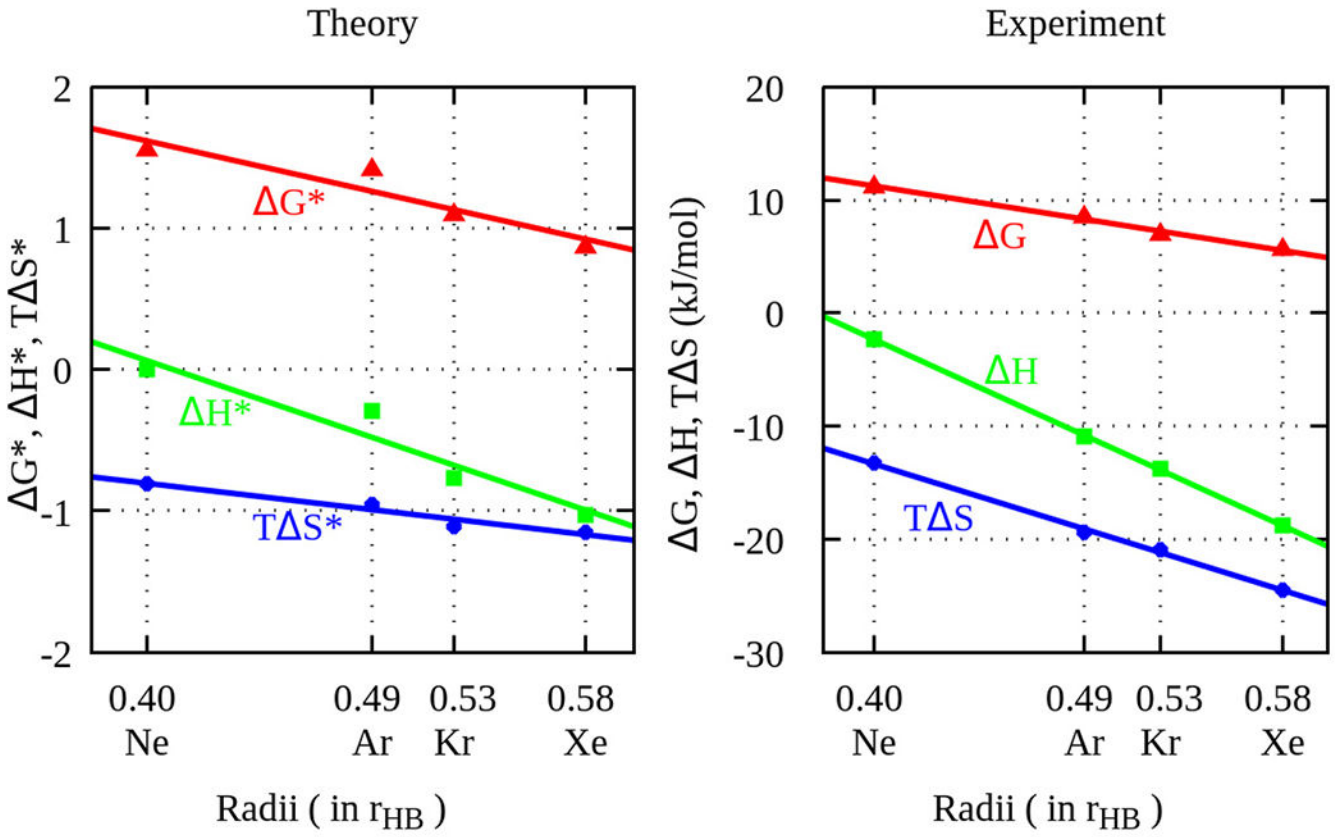

Figure 7.

Nonpolar hydration vs solute radius, from theory and experiments at a fixed temperature, for theory at 0.17 in reduced units and for the experiment at 25 °C.

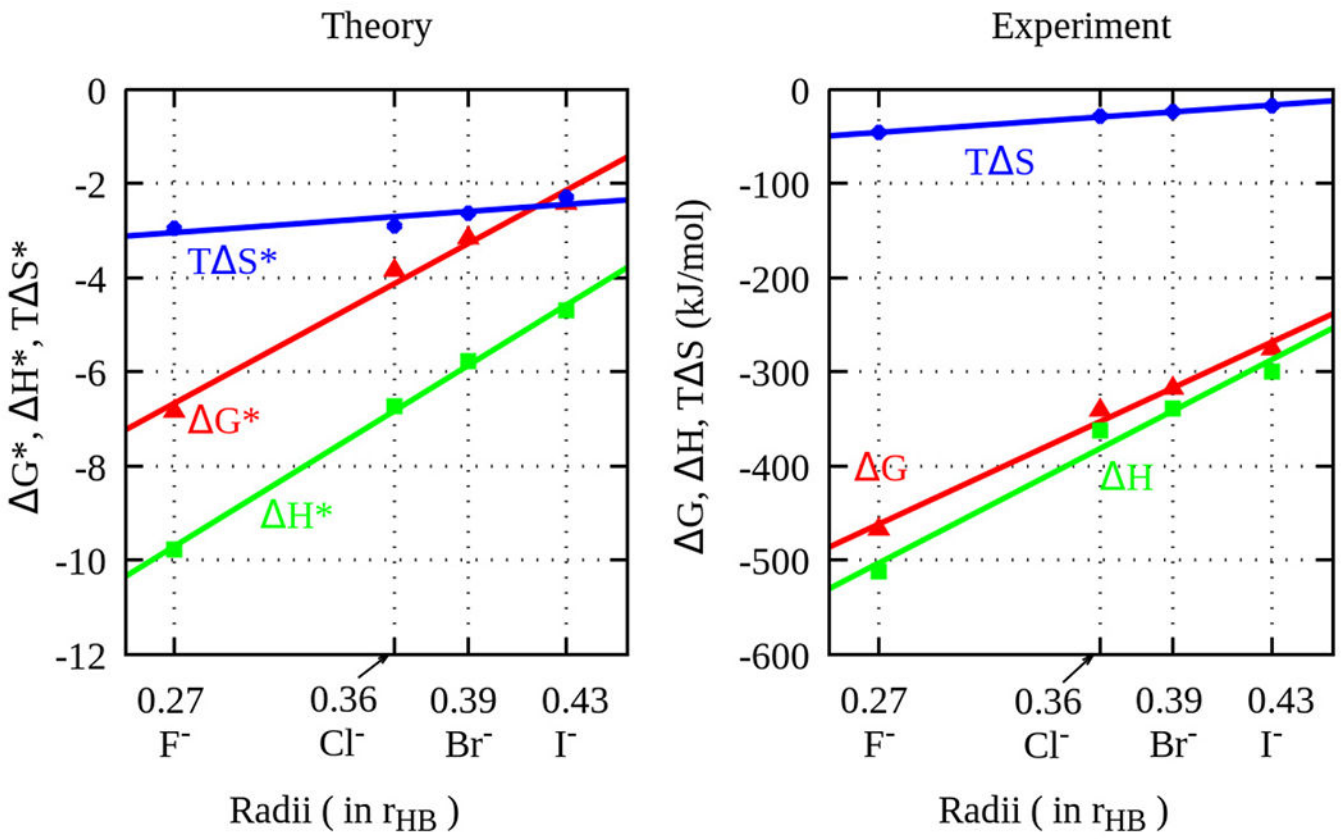

Figure 8.

Anion hydration as a function of solute radii. Theoretical results are shown in reduced units (T^* = 0.15). Experiments are at 25 °C.

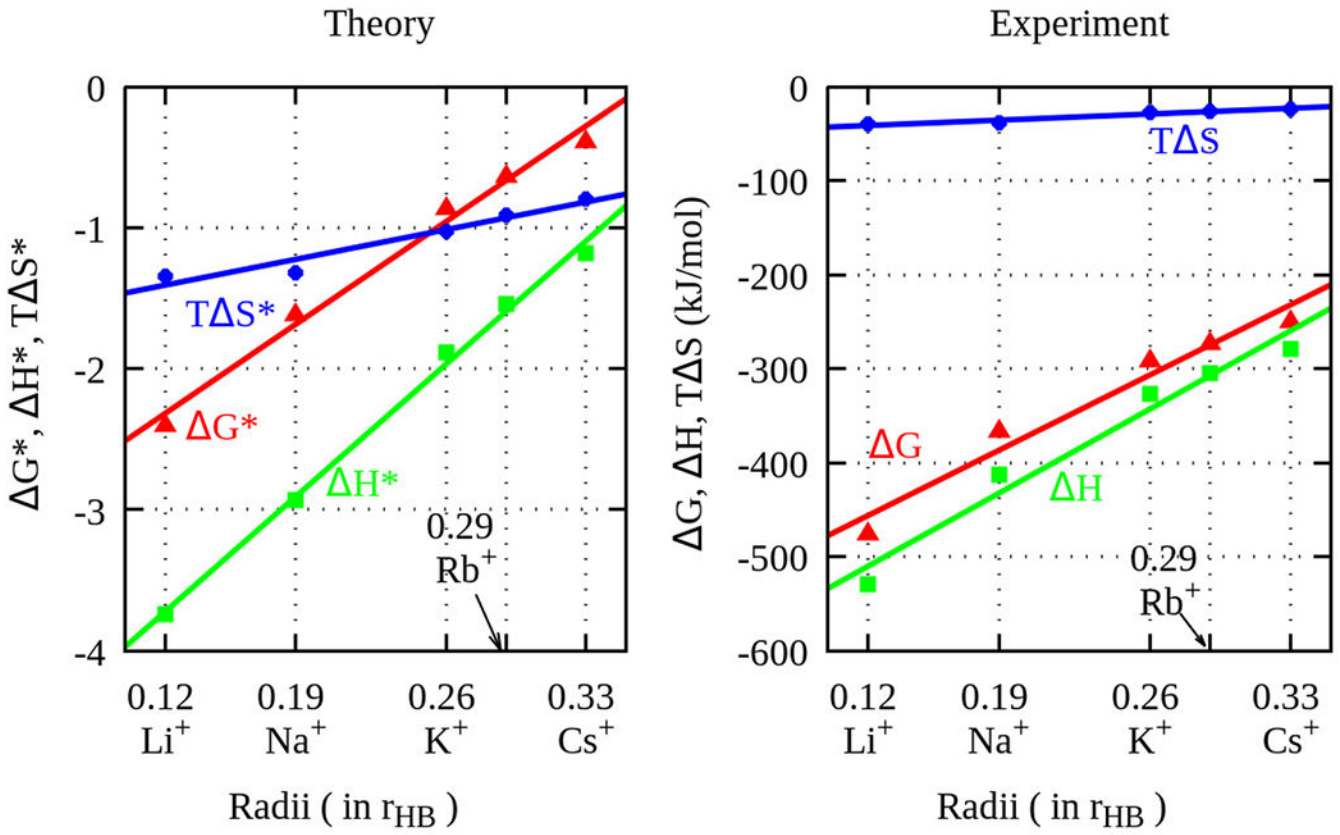

Figure 9.

Cation hydration as a function of solute radii. Theoretical results are shown in reduced units (T^* = 0.15). Experiments are at 25 °C.

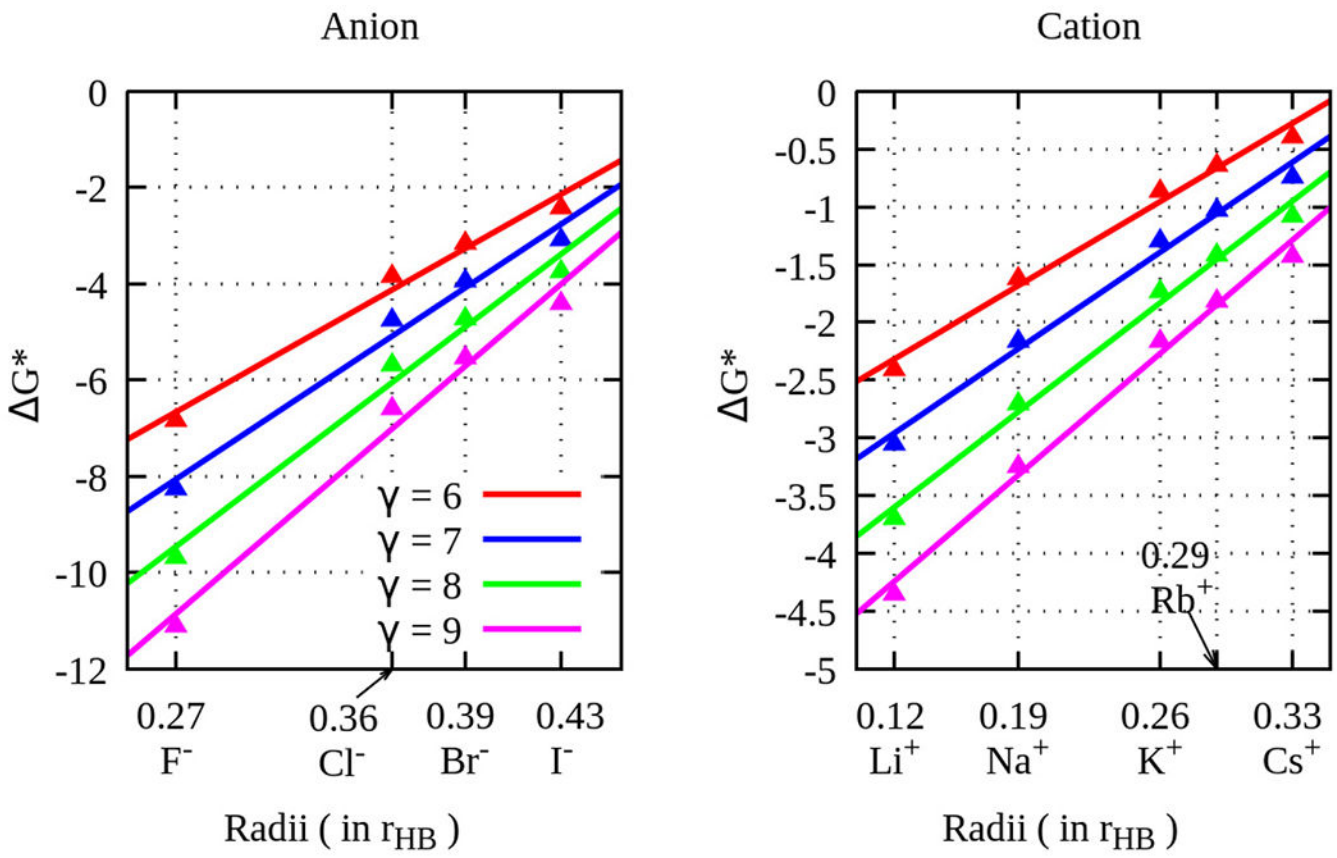

Figure 10.
Effect of varying the parameter γ on the ion hydration free energy as a function of solute radii.

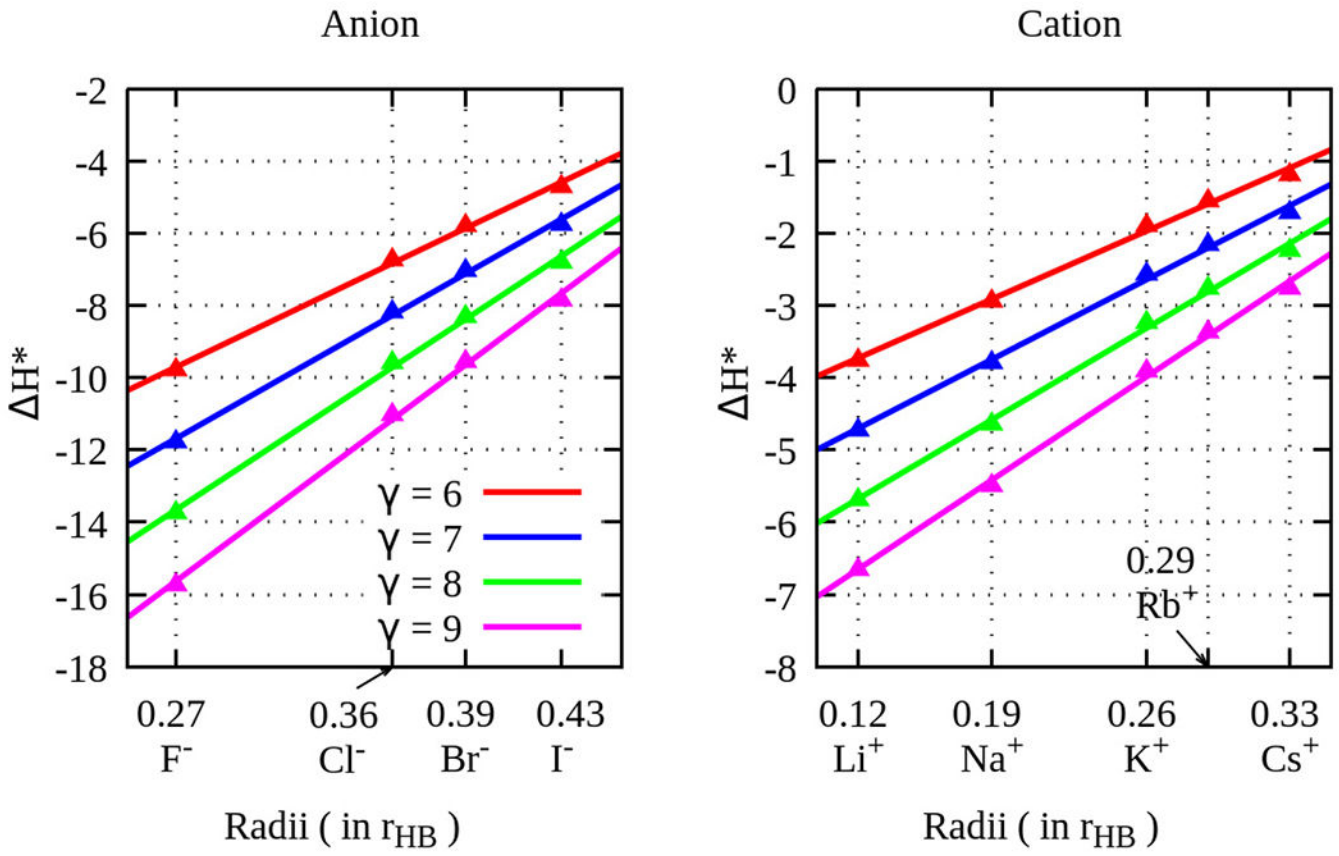

Figure 11.
Effect of varying the parameter γ on the ion hydration enthalpy as a function of solute radii.

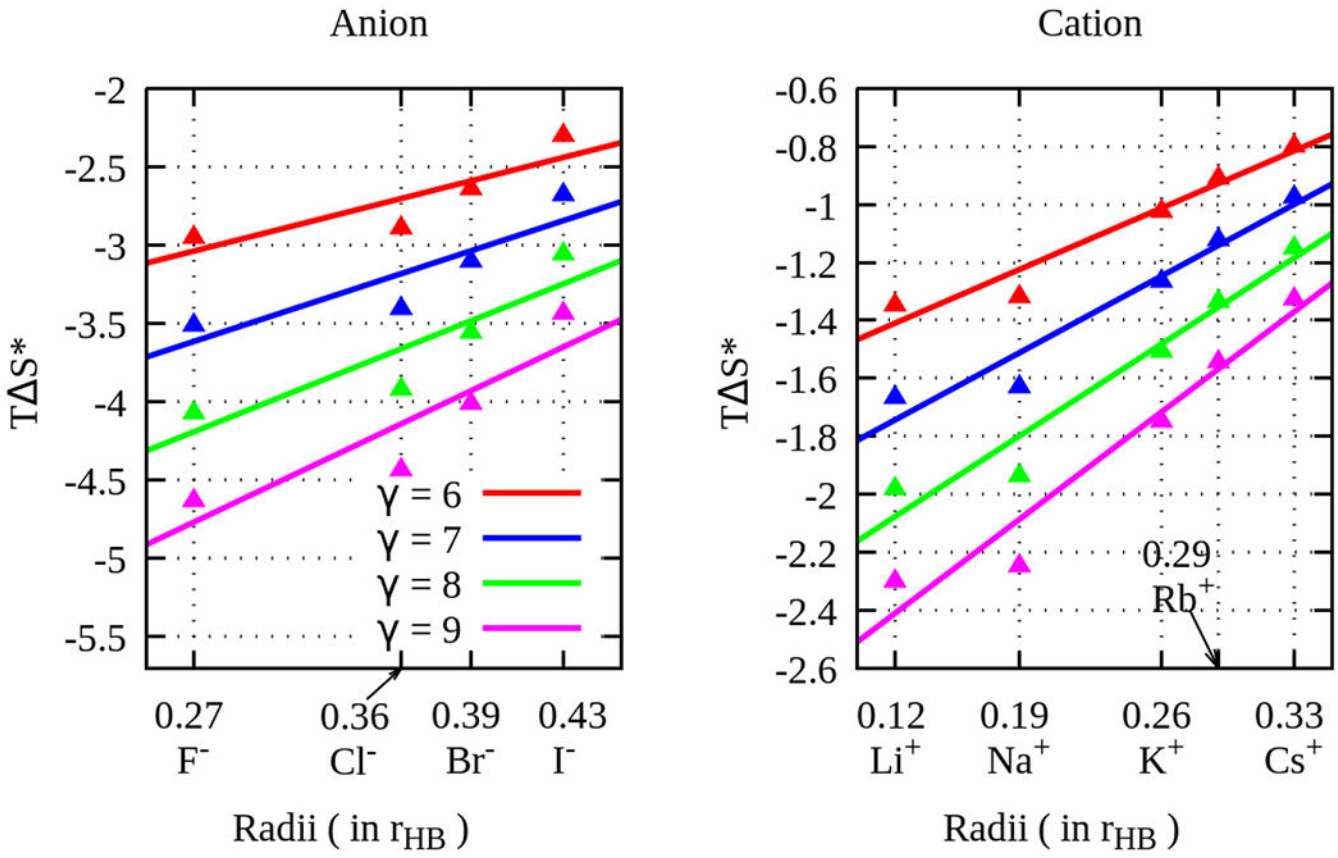

Figure 12.
Effect of varying the parameter γ on the ion hydration entropy as a function of solute radii.

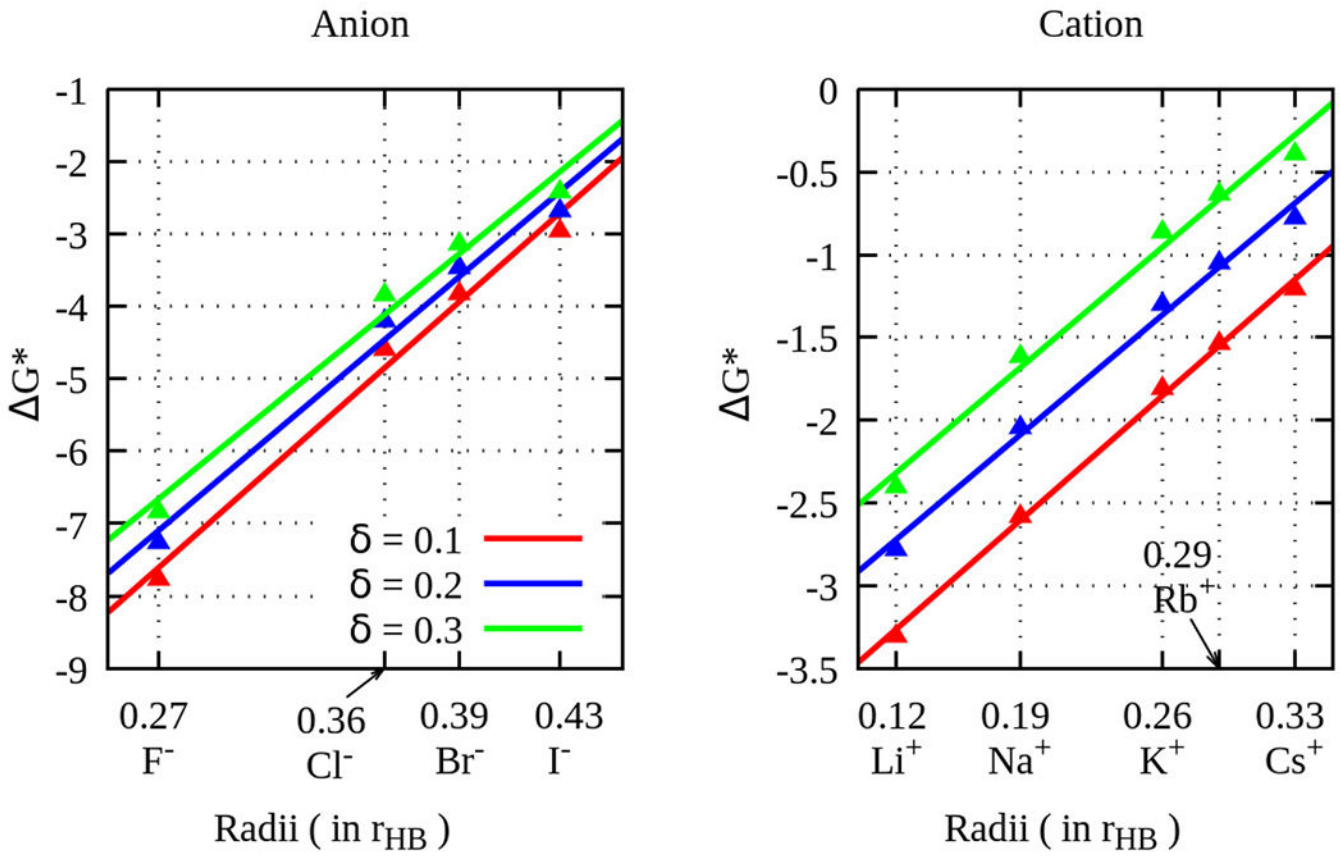

Figure 13.
Effect of varying the parameter δ on the ion hydration free energy as a function of solute radii.

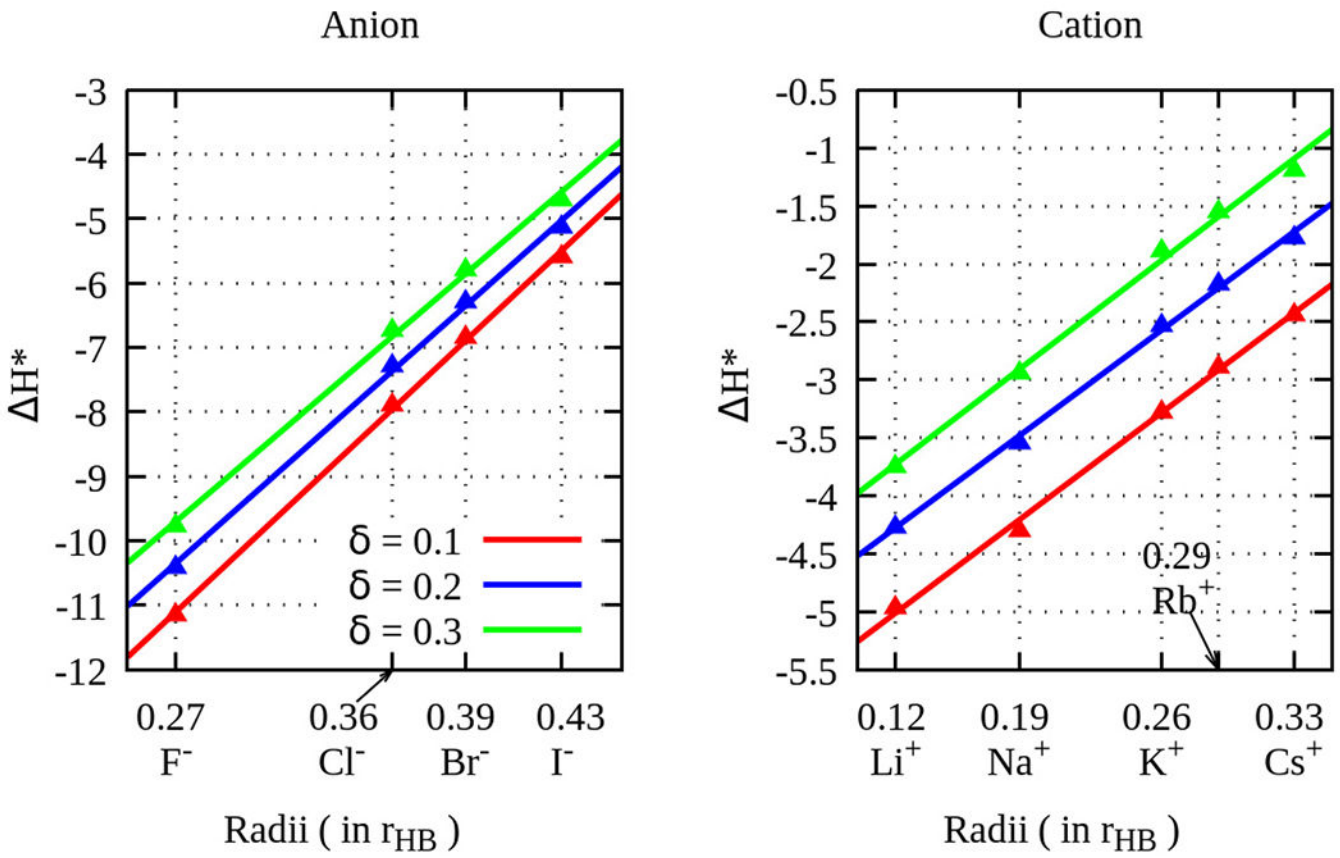

Figure 14.
Effect of varying the parameter δ on the ion hydration enthalpy as a function of solute radii.

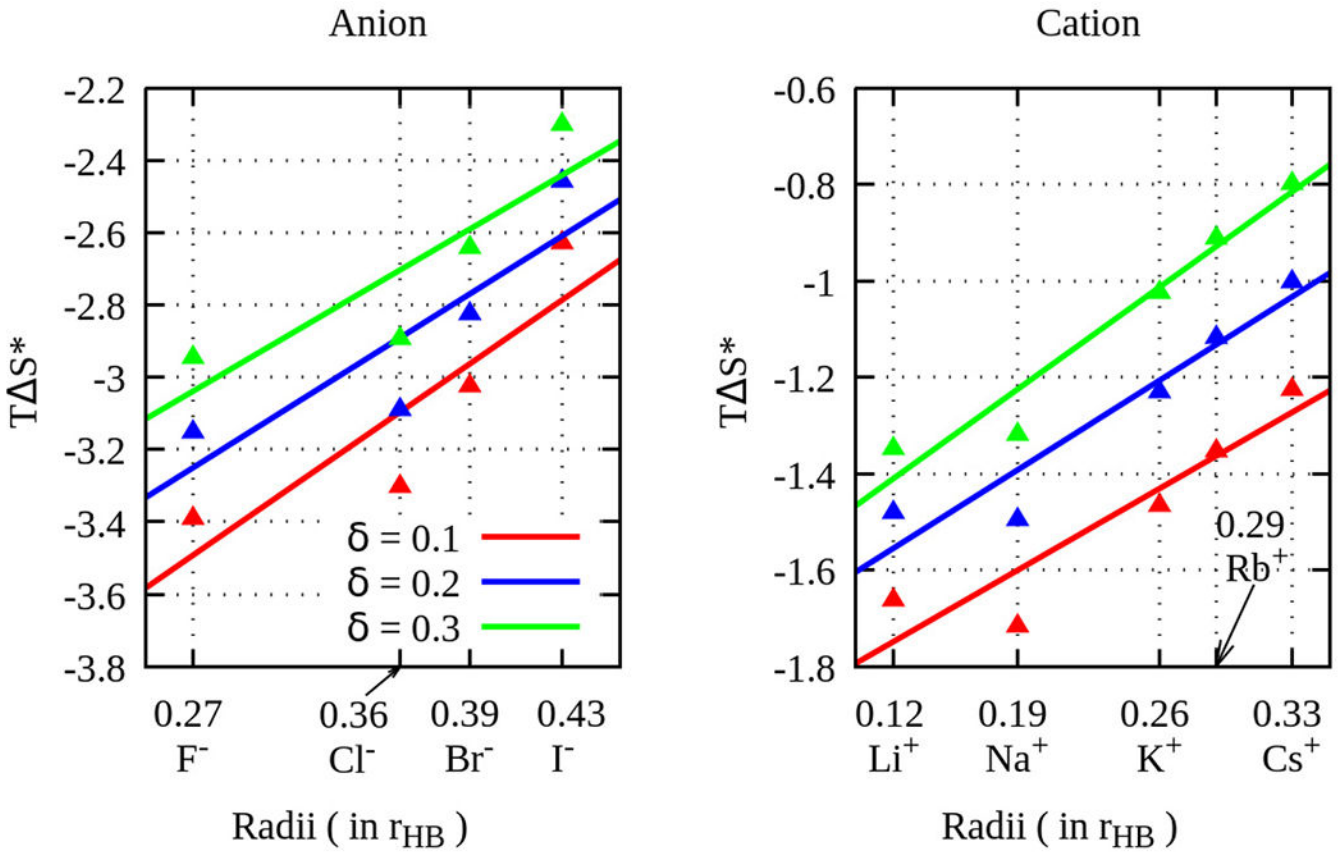

Figure 15.
Effect of varying the parameter δ on the ion hydration entropy as a function of solute radii.

Table 1.

Ion Diameters Used in the Calculation (in Reduced Units) and the Experimental Thermodynamic Quantities[a]

ion	diameter used	Δ*G*	Δ*H*	Δ*S*
Li^+	0.24	−475.6	−528.9	−131.2
Na^+	0.37	−365.8	−413.0	−129.8
K^+	0.52	−295.2	−331.2	−93.6
Rb^+	0.58	−273.0	−304.2	−85.8
Cs^+	0.66	−249.6	−278.4	−76.8
F^-	0.53	−467.2	−512.0	−153.6
Cl^-	0.71	−340.4	−362.6	−96.2
Br^-	0.77	−316.8	−338.4	−79.2
I^-	0.85	−275.4	−291.6	−56.7

[a]Key: hydration free energy, Δ*G*, hydration enthalpy, Δ*H*, and hydration entropy, Δ*S*, obtained at 25C and 1 atm pressure. Δ*G* and Δ*H* are in kJ/mol. Δ*S* is in J/K/mol. The experimental data were taken from ref 34.